16A.3 SYNOPTIC ENVIRONMENTS AND CONVECTIVE MODES ASSOCIATED WITH SIGNIFICANT TORNADOES IN THE CONTIGUOUS UNITED STATES

Richard L. Thompson* and Jeremy S. Grams
Storm Prediction Center
Norman, OK

Jayson A. Prentice
Iowa State University
Ames, IA

1. INTRODUCTION

Tornado forecasting has evolved considerably since the formation of the Severe Local Storms (SELS) Center of the United States Weather Bureau in the early 1950s (Winston 1956), to the current variation of SELS known as the Storm Prediction Center (SPC). Forecasting in the early days of SELS was limited largely to pattern recognition, sounding analysis, and subjectively predicting changes in the convective environment (Schaefer 1986; Galway 1992). More recent advances in numerical modeling and detailed field observations have resulted in greater physical understanding of the processes supportive of severe thunderstorms and tornadoes (see the reviews by Bluestein 1999, Davies-Jones et al. 2001, and Wilhelmson and Wicker 2001). This increasing knowledge base has manifested itself in a more "ingredients-based" approach (Doswell et al. 1996) to severe storm forecasting focusing on parameters representing relevant physical processes (Johns and Doswell 1992; Moller 2001), and led to numerous observational studies aimed at identifying environmental characteristics associated with various types of severe thunderstorms and tornadoes (e.g., Johns et al. 1993, Rasmussen and Blanchard 1998, and Thompson et al. 2003 among others).

Convective mode has received increasing attention in recent years as regional and local radar data allow identification of primary storm types associated with reported tornadoes. Trapp et al. (2005) examined all reported tornadoes from January 1998 through December 2000 and associated radar reflectivity mosaics to establish the relative frequency of tornadoes with quasi-linear convective systems (QLCS). Their results suggest that QLCSs are responsible for as much as 35-50% of all tornadoes in the Midwest (e.g., Indiana and surrounding states), and that QLCS tornadoes occasionally produce damage rated F2-F4 (EF2-EF4 in the enhanced Fujita scale). However, operational meteorologists at the SPC, as well as long-time storm enthusiasts, have noted a distinct tendency for significant tornadoes (F2-F5 damage) in the Plains to occur with discrete supercells as opposed to linear convective systems. Convective mode has been considered an important ingredient in forecasts of significant severe storm events (Thompson and Mead 2006), but the climatological distribution of significant tornadoes with respect to convective mode has been based more on individual case studies or anecdotal evidence than documented samples.

Operational meteorologists have benefited from a dramatic increase in the quantity and quality of numerical weather prediction model guidance since the mid 1990s with the advent of gridded model output and numerous derived model parameters related to severe storm occurrence (e.g., measures of buoyancy and vertical shear). However, standard pressure level displays are still utilized amongst operational meteorologists, and it is these standard fields that form the initial basis for many severe storm forecasts. Still, the distributions of mandatory pressure level winds, temperatures, moisture, and geopotential heights in tornado episodes over the contiguous United States have not been re-examined since the 1970s (e.g., Miller 1972, David 1976). Our intention here is to document all significant tornadoes from 2000-2007, when NEXRAD radar data have been widely available, and to catalog a set of environmental variables that have been used through the past 25-50 years as part of the approach to tornado forecasting.

The ultimate goal is to help operational forecasters calibrate their own personal observations and preferences regarding synoptic pattern recognition and convective mode when attempting to forecast significant tornadoes.

2. CASE SELECTION METHODOLOGY AND CRITERIA

All F2+ tornado occurrences in the contiguous United States were identified from January 2000 through December 2007. We restricted our examination to F2+ tornadoes because such events are more likely to be reported properly as tornadoes (compared to weak tornadoes with less distinct damage patterns and radar signatures), and F2+ tornadoes are responsible for the vast majority of tornado injuries and fatalities. Of course, any particular tornado event is subject to the vagaries of damage ratings (Doswell and Burgess 1988). For each tornado, the convective mode was determined at the beginning time of the tornado report, utilizing base (0.5o elevation angle) radar reflectivity mosaic images available from either the SPC severe thunderstorm events page (http://www.spc.noaa.gov/

*Corresponding author address: Richard L. Thompson, 120 David L. Boren Blvd., Norman, OK 73072. Email: richard.thompson@noaa.gov

exper/archive/events/) or the image archive from the University Center for Atmospheric Research (http://locust.mmm.ucar.edu/case-selection/). Three convective mode possibilities were defined as follows:

1. Discrete cell - Relatively isolated cell(s) with a circular or elliptically shaped region of reflectivity with maximum values greater than or equal to 50 dBZ, after Trapp et al. (2005).

2. QLCS - A continuous major axis of at least 40 dBZ echoes with length greater than or equal to 100 km that shared a common leading edge and moved in tandem. In addition, the major axis had to be at least three times as long as the minor axis, following Trapp et al. (2005) and Grams et al. (2006).

3. Cluster - Reserved for conglomerates of several cells that were not clearly identifiable as either discrete or QLCS in regional radar reflectivity mosaics; typically consisting of at least a contiguous region of 40 dBZ echoes in a 2500 km2 (i.e., 50 X 50 km) area.

The discrete cell and QLCS events were relatively easy to identify in most cases, as illustrated in Fig 1. Neither individual WSR-88D site data nor algorithm output was utilized in convective mode determination for each case. Several of the cluster and QLCS categorizations may have consisted of more discrete supercell components when considering full resolution (level II) reflectivity and velocity data. However, given the necessarily subjective nature of convective mode categorizations, we believe examination of the simple base reflectivity mosaic images was sufficient to correctly identify the vast majority of events. The most significant tornadoes (i.e., greatest F-scale or EF-scale damage rating) were catalogued during each convective day (12 UTC – 12 UTC) for each of the three convective modes, and these tornadoes served as the basis for additional data collection. The total number of significant tornadoes attributable to the three convective modes was also identified for each convective day.

Synoptic and mandatory pressure level data were only cataloged for the greatest F-scale/EF-scale damage rated significant tornadoes with each convective mode type. Additional F2+ tornadoes that occurred within 6 hours of the most significant tornado with each mode type, and within the same region of convection (assessed subjectively), were not considered as separate events. Mandatory pressure level and surface data (Table 1) were interpolated bi-linearly to the initial time and location of the most significant tornado for each convective mode during the convective day. For example, multiple significant tornadoes with multiple discrete cells were often considered a single case in this sample. This approach reduced the chance that single outbreaks with many significant tornadoes would dominate the results and introduce data dependency into the sample (i.e., redundant data for multiple tornadoes in close proximity).

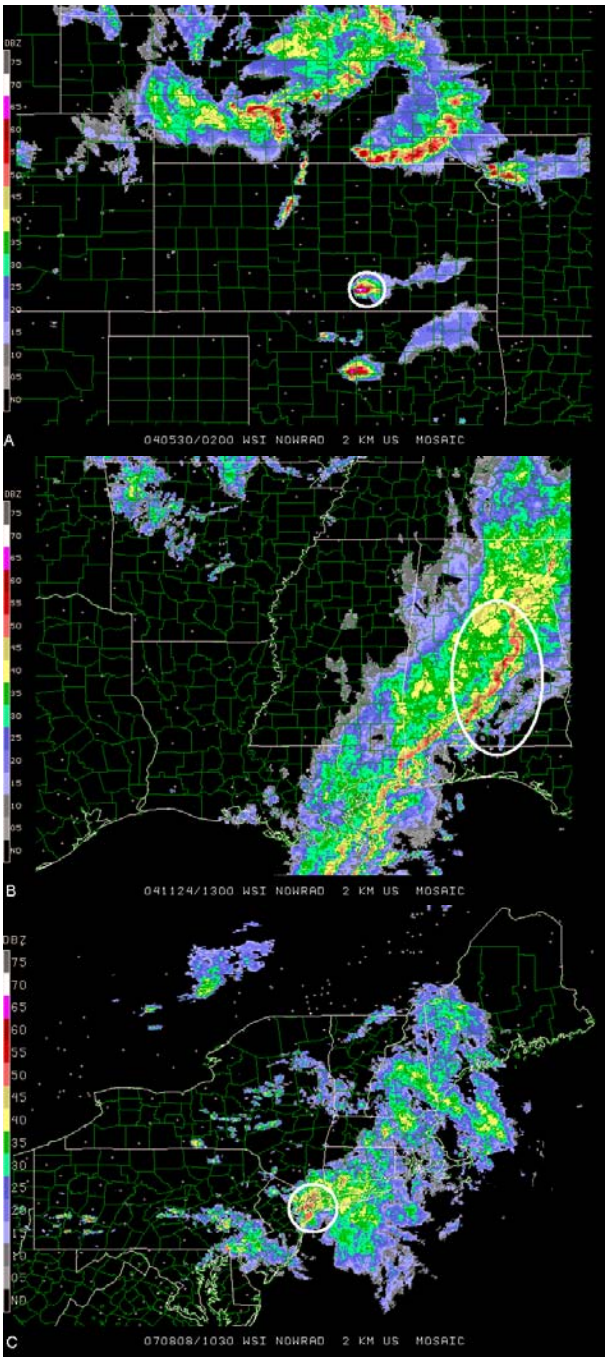

Figure 1. Examples of convective modes derived from regional reflectivity mosaic images: a) discrete cell, b) QLCS, and c) cluster.

Representative surface conditions were interpolated to the time and location of each significant tornado case. Any synoptically evident boundaries were noted in proximity to each case, as well as surface boundaries at the time and location of storm initiation. Boundary identification did not include satellite or radar imagery, thus small-scale or subtle boundaries may not be included in our sample.

Table 1. List of mandatory pressure level and surface parameters collected by RUC model or subjective analysis.

Parameter	300 hPa	500 hPa	700 hPa	850 hPa	Surface
Dew Point				X	X
Geopotential Height		X			
Sea Level Pressure					X
Temperature	X	X	X	X	X
Wind Direction	X	X		X	
Wind Speed	X	X		X	

Table 2. Difference between RUC analysis and subjectively interpolated data for selected parameters on 219 identical cases from May 2002-Dec 2007

500 hPa Geopotential Height
Mean difference: 9 m

Difference threshold	Number of cases	Percentage of cases	Cumulative percentage
± 10 m	99	45%	
± 20 m	67	31%	76%
± 30 m	33	15%	91%
> 30 m	20	9%	

500 hPa Wind Direction
Mean difference: -2.2°

Difference threshold	Number of cases	Percentage of cases	Cumulative percentage
± 11.25°	150	68%	
± 22.50°	52	24%	92%
> 22.50°	17	8%	

700 hPa Temperature
Mean difference: 0.0°C

Difference threshold	Number of cases	Percentage of cases	Cumulative percentage
± 1°C	173	79%	
± 2°C	37	17%	96%
> 2°C	9	4%	

850 hPa Dew Point
Mean difference: 0.1°C

Difference threshold	Number of cases	Percentage of cases	Cumulative percentage
± 1°C	121	55%	
± 2°C	50	23%	78%
± 3°C	23	11%	89%
> 3°C	25	11%	

850 hPa Wind Speed
Mean difference: -0.3 m s-1

Difference threshold	Number of cases	Percentage of cases	Cumulative percentage
± 2.5 m s-1	110	50%	
± 5.0 m s-1	76	35%	85%
± 7.5 m s-1	18	8%	93%
> 7.5 m s-1	15	7%	

Beginning in May 2002, mandatory pressure level data were collected from the NCEP operational RUC model (Benjamin et al. 2004) hourly analyses at the nearest grid point for each tornado event. The 40-km RUC model gridded analyses were utilized from May 2002 through December 2004, with the 20-km analyses available thereafter. From January 2000 through April 2002, upper air data were interpolated subjectively to the time and location of each tornado event from a combination of the raw data plots and objectively contoured fields in the archived charts (00 and 12 UTC) on the SPC web page. A tornado event was omitted from our sample if any archived charts were missing. The case data were also interpolated for all of the tornado events from May 2002 through December 2007 to form a comparison sample between the objective RUC analyses and the subjectively interpolated data. Differences between the two data retrieval methods

were generally small with negligible biases (see Table 2). Thus, the subjectively interpolated data were used to extend the tornado event sample by another 101 cases back to January 2000.

3. PRELIMINARY RESULTS

a) Geographic and temporal distribution of significant tornado cases

A total of 359 significant tornado cases were collected during the eight year period from January 2000 through December 2007 across the contiguous United States. The significant tornado cases in our sample represented 864 individual significant tornadoes. As shown in Fig. 2, the relative frequency of significant tornadoes with discrete cells was greater (74%) than the representation of discrete cell cases (64%).

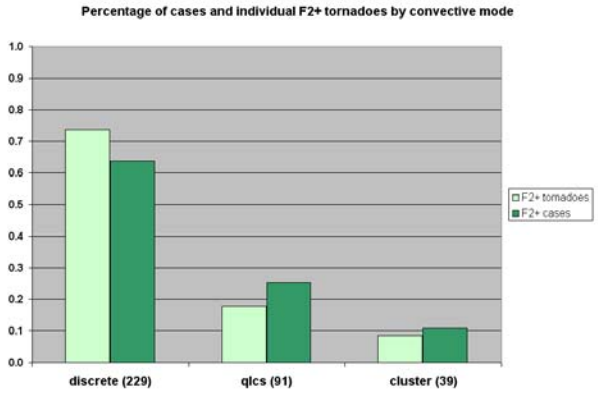

Figure 2. Relative frequency of significant tornadoes by convective mode comparing the percentage of total tornadoes to the percentage represented in the case sample (in parentheses.).

QLCS tornadoes were somewhat over-represented in the case selection process (25% of the cases compared to only 18% of the tornado total). Larger outbreaks of significant tornadoes with discrete storms are more common than similar outbreaks of significant QLCS tornadoes, and our sample may be skewed slightly in favor of the QLCS cases. Approximately 10% of the cases and significant tornadoes were produced by clusters. The relative distributions of significant tornadoes increasingly favor discrete cells over QLCSs when tornado damage ratings increase from F2 to F4 or greater (Fig. 3). Our sample of significant tornadoes agrees with the findings of Trapp et al. (2005) where cells produced 79% of all tornadoes, while QLCSs produced 18% of the tornadoes.

The selected cases were concentrated between the Rockies and the Appalachians (Fig. 4). Significant tornado cases were substantially less common across the high Plains states from New Mexico to Montana, though low population densities and few structures suggest that a larger percentage of high Plains tornadoes may be under-rated or under-reported compared to areas farther east in the Plains and Mississippi Valley (e.g., Rasmussen 2003). Relatively few significant tornado cases were documented from the central Appalachians into New England. Only two significant tornadoes occurred during the eight year period across the western United States, and regional reflectivity mosaics were not available for those two events.

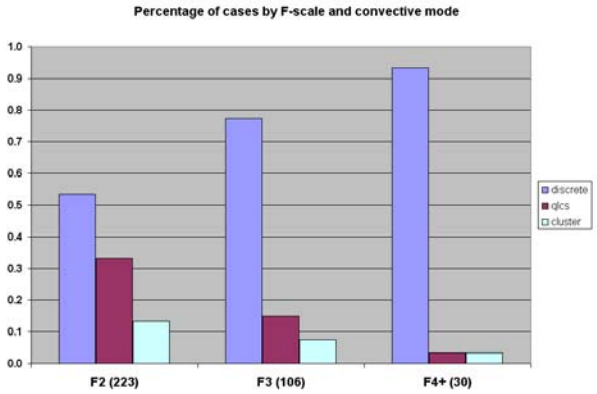

Figure 3. Relative frequency of convective mode by F/EF-scale in the case sample (in parentheses).

Regional subdivisions marked in Fig. 4 were based on geographic features (e.g., the Rockies and Appalachians), variations in seasonal flow regimes (e.g., the Southern Plains versus the Northern Plains in the summer), and climatological variations in significant tornado environments (e.g., low-level flow direction and resultant moisture distributions from the Southern Plains to the Southeast). In the case of Michigan, it was included in the "Midwest" region since the majority of the significant tornado cases occurred in southern Lower Michigan as an extension of related events in neighboring Indiana.

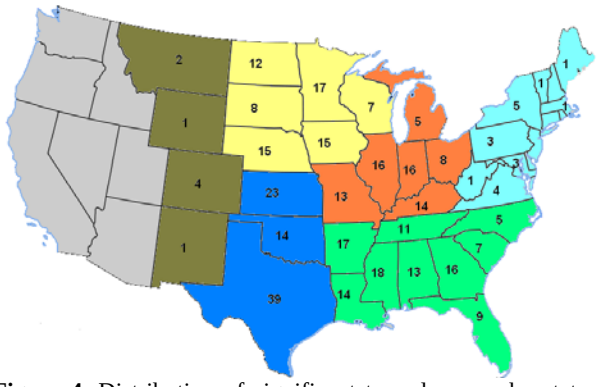

Figure 4. Distribution of significant tornado cases by state. Geographic regions are noted in the color-filled groupings by state (Southern Plains [SP, blue], Northern Plains [NP, yellow], Midwest [MW, orange], Southeast [SE, green], Northeast [NE, cyan].

Convective mode varied notably by season, with a clear majority of spring (Mar-May) and summer (Jun-Aug) significant tornado cases associated with discrete cells (Fig. 5). Significant tornado cases with QLCSs also peaked in the spring, though at much lower

frequencies compared to discrete cells. Significant tornado cases with QLCSs varied by roughly a factor of two across all four seasons, compared to a factor of five for discrete cell cases. The convective mode associated with significant tornadoes in the winter, when the frequency of QLCS and discrete cell cases were nearly identical, differed substantially from other seasons.

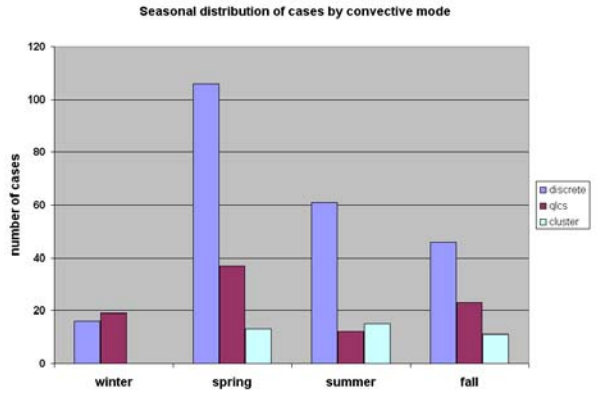

Figure 5. Seasonal distribution of convective mode in the case sample.

Marked differences were noted in the temporal distributions of significant tornadoes within the warm season (Apr-Oct, Fig. 6a). A 3-h running mean was applied to each hour to damp sampling vagaries and maintain the more prominent signals in the data (after Trapp et al. 2005). The discrete cell cases exhibited a pronounced diurnal cycle with a sharp peak in events near 00 UTC. The QLCS significant tornado cases displayed a similar diurnal maximum at a much lower magnitude. Interestingly, a small secondary peak in QLCS significant tornadoes occurred near 09 UTC, or around the same time as the relative minimum in discrete cell cases. Cool season cases (Nov-Mar, Fig. 6b) were substantially less frequent than during the warm season, and the diurnal peak in discrete cells was much less pronounced. The QLCS tornado cases were much more evenly distributed from late afternoon through mid morning hours. The absolute minimum in QLCS cases corresponded to a relative maximum in discrete cell cases during the cool season at 20 UTC. This minimum in QLCS cases may be a result of organized convective systems dissipating in the morning, and prior to the upscale growth of new convective systems later in the afternoon and evening. The distinct lack of a diurnal cycle with the QLCS significant tornado cases is the most noteworthy difference compared to the discrete cell cases.

A further regional and seasonal breakdown in cases reveals several important differences in convective mode and significant tornado production. From Figs. 7a and 7b, it is seen that a vast majority of Southern Plains significant tornado cases occurred with discrete cells during the spring (Mar-May), with a similar signal across the Northern Plains in the summer.

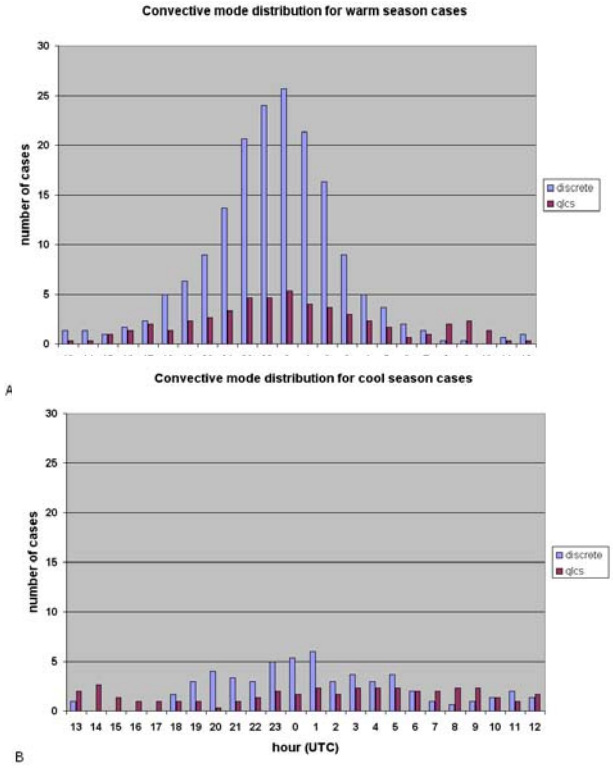

Figure 6. Three-hour running mean of significant tornado cases by hour (UTC) for a) the warm season [Apr-Oct], and b) the cool season [Nov-Mar].

Significant tornado cases were also more common with discrete cells across the Midwest in the spring, though QLCS significant tornado cases occurred at nearly the same frequency in the Southeast in the spring and fall (Sep-Nov). The peak for discrete cell significant tornado cases during the fall in the Southeast was likely a result of the large number of intense hurricane landfalls and associated tornado cases in 2004 and 2005. Differences in convective mode frequency between the winter and spring were minimal in the Southeast.

The largest tornado outbreaks (i.e., six or more F2+ tornadoes) were characterized by the greatest percentage of significant tornadoes with discrete cells (79% of 406 individual tornadoes), and substantially fewer QLCS (16%) and cluster events (5%). Convective days with a single significant tornado were more commonly the result of QLCSs and clusters (31% and 14% of 108 individual tornadoes, respectively), though discrete cells still produced a majority of the isolated significant tornadoes (55%).

b) Synoptic pattern data

Miller (1972) noted several mandatory pressure level and surface parameters associated with significant

severe weather outbreaks. Similar mandatory pressure level and surface data (Table 1) were collected from RUC model or subjective analyses. Each case was assigned into geographical and seasonal categories as described in section 3a. In addition, a comparison was performed of events with six or more significant tornadoes versus a singular F2 or EF2.

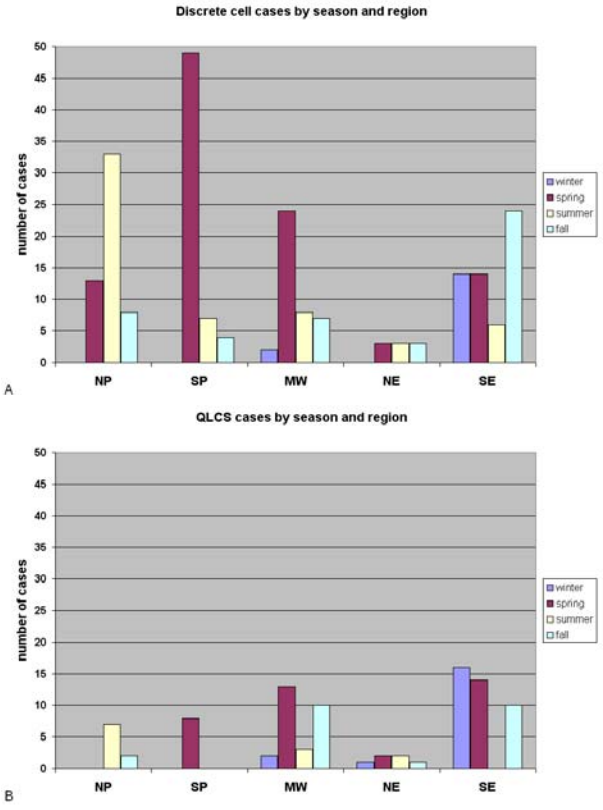

Figure 7. Regional and seasonal breakdown of significant tornado cases with a) discrete cells, and b) QLCSs.

i) Winds and heights

The mean 500 (850) hPa wind direction for all cases was from 235° (204°). Mid-level flow was clustered around the southwest direction (225°) in the Southeast region during fall and winter, compared to having a more westerly component in the spring (Fig. 8a). Other than the Southeast region experiencing southwesterly flow during the fall and winter, the 500 hPa wind direction for the peak frequency of significant tornado cases in other regions was generally from the west-southwest. Flow at 850 hPa was typically more southerly in the Southern Plains during spring compared to the Midwest and Southeast region (Fig. 8b). Fall cases in the Southeast region tended to have more southerly 850 hPa winds compared to spring and winter, perhaps a reflection of the influence of tropical cyclones during this period.

The mean 500 (850) hPa wind speed for all events was 27 (19) m s-1. Figs. 9a and 9b depict substantially weaker 500 and 850 hPa winds in Northern Plains summer cases compared to all other regions and seasons. This corresponds to the annual oscillation in location and amplitude of the polar westerlies over the United States, and the relationship of the polar jet to the low-level jet in severe weather situations (e.g., Uccellini and Johnson 1979). Overall wind speeds were generally lower in events across the Plains compared to the southeast region and Midwest. However, comparing Figs. 8a and 8b, greater veering of the wind profile can be inferred in cases over the Plains. This suggests both speed and direction play important roles for determining the magnitude of deep-layer shear in the Plains; whereas more unidirectional and stronger kinematic profiles characterize the Southeast region and Midwest. Both low and mid-level flow tended to be stronger in cases with six or more significant tornadoes compared to a singular F2 or EF2 (Figs. 10a and 10b), suggestive of a more amplified synoptic pattern or stronger mean flow during robust significant tornado days. These findings agree with the proximity sounding work of Markowski et al. (2003) where significantly tornadic supercell events were characterized by stronger ground-relative winds compared to nontornadic supercell events.

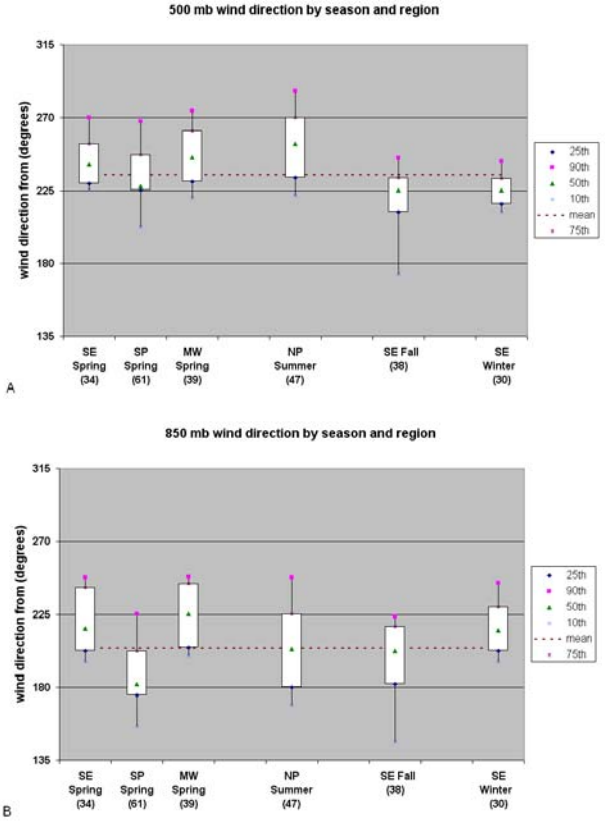

Figure 8. Box and whiskers plot of percentile rank distributions of wind direction by region and season for a) 500 hPa and b) 850 hPa, with the number of cases listed below each category. The dashed horizontal line marks the mean value for the entire sample.

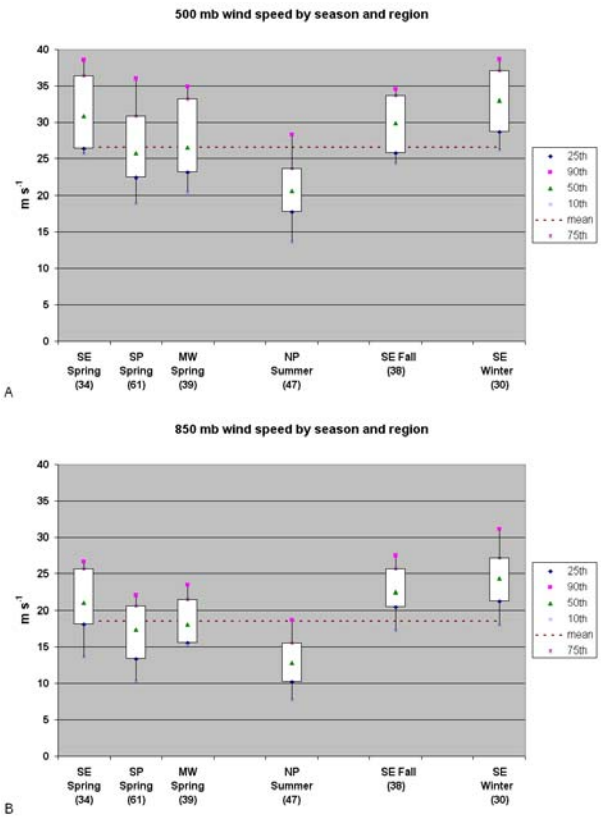

Figure 9. Same as in Fig. 8, except for wind speed.

David (1976) collected a large sample of interpolated mandatory level variables for every tornado during the period 1968-1974. Wind directions at 850 and 500 hPa were similar in his Table 2 compared to ours (Table 3), even though we considered only significant tornado cases. Differences are more pronounced in the wind speeds, where our sample reveals substantially stronger speeds at all levels across all seasons. The differences in wind speeds between the two samples were less pronounced, but still of the same sign, when considering only David's "maxi" tornado cases (path length 10 mi or more, his Table 5).

These differences likely arise from variations in the tornado data samples (all tornadoes versus only significant tornadoes), and the increased spatial and temporal resolution of RUC analyses which dominated our case sample.

The mean 500 hPa height fall for significant tornado cases (tornado time minus 12 hours) for the sample was 30 meters. Falls were most pronounced over the Southeast region during winter, and smallest over the Northern Plains region in summer (Fig. 11a). Height falls tended to be somewhat greater for cases with higher number of significant tornadoes versus one F2 or EF2 (Fig. 11b). Both of these trends are consistent with the differences in 500 hPa wind speeds noted previously. Interestingly, almost half of all cases were characterized by only small 500 hPa height falls, or small height rises (especially during the Northern Plains summer). It should be noted that the height changes described here refer to the immediate vicinity of the tornado cases, while greater upstream height falls may be associated with the synoptic systems.

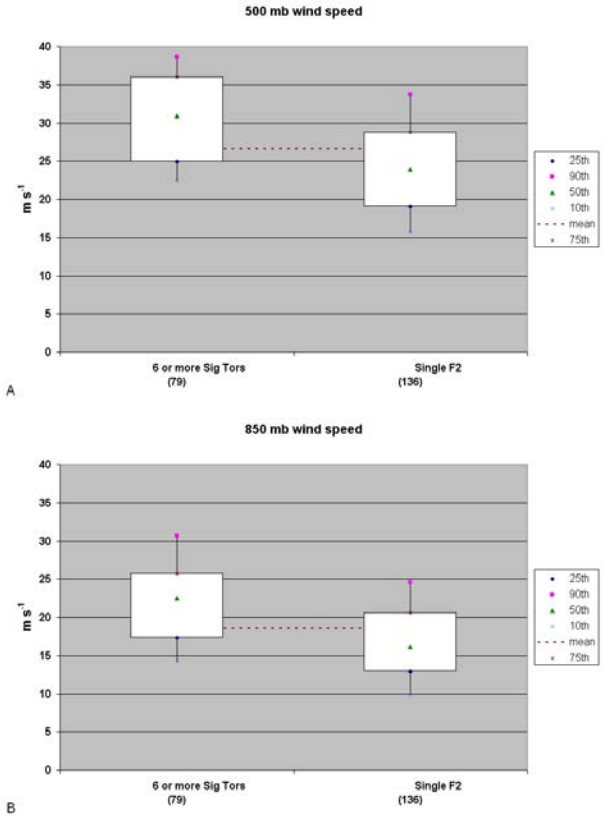

Figure 10. Same as in Fig. 9, except for cases with six or more significant tornadoes versus a single F2/EF2.

ii) Temperature and dew point

The mean 500, 700, and 850 hPa temperatures for all cases were -11°, 6°, and 16° C, respectively, which are in good agreement with David (1976, his Table 2). In general, warmer temperatures in the summer over the Northern Plains and cooler temperatures in the winter over the Southeast region (Figs. 12a and 12b) are consistent with the annual variation of the low to mid-tropospheric thermodynamic profile. The mean 850 hPa dew point for all cases was 13° C. Our dew point values were roughly 4 ° C greater across all seasons than those found by David (1976). The greatest regional/seasonal difference is between the Northern Plains summer and Southeast winter (Fig. 13a), with this trend also consistent in 850 hPa temperatures (not shown). Despite this difference, the mean change in 850 hPa dew point of 3.4°C from 12-h prior to initial tornado time was consistent across all regions and seasons (Fig. 13b).

Table 3. Means and standard deviations by geographical and temporal categories of selected parameters, adapted from David (1976).

Parameter	SE Spring	SP Spring	MW Spring	NP Summer	SE Fall	SE Winter
850 hPa Temperature (°C)	15	17	15	17	15	12
SD (standard deviation)	2	3	3	3	2	2
850 hPa Dew Point (°C)	13	13	12	13	13	10
SD	3	3	3	3	2	2
850 hPa DIR (deg)	220	191	224	191	197	217
SD	23	27	24	27	30	18
850 hPa Speed (kt)	41	33	37	33	43	48
SD	10	9	8	9	8	10
700 hPa Temperature (°C)	5	7	5	7	6	3
SD	2	3	3	3	3	2
500 hPa Temperature (°C)	-12	-12	-13	-12	-10	-14
SD	2	3	3	3	3	3
500 hPa DIR (deg)	243	233	246	233	218	225
SD	17	23	25	23	27	13
500 hPa Speed (kt)	61	52	53	52	57	64
SD	12	14	11	14	10	10
Number of cases	34	61	39	7	38	30

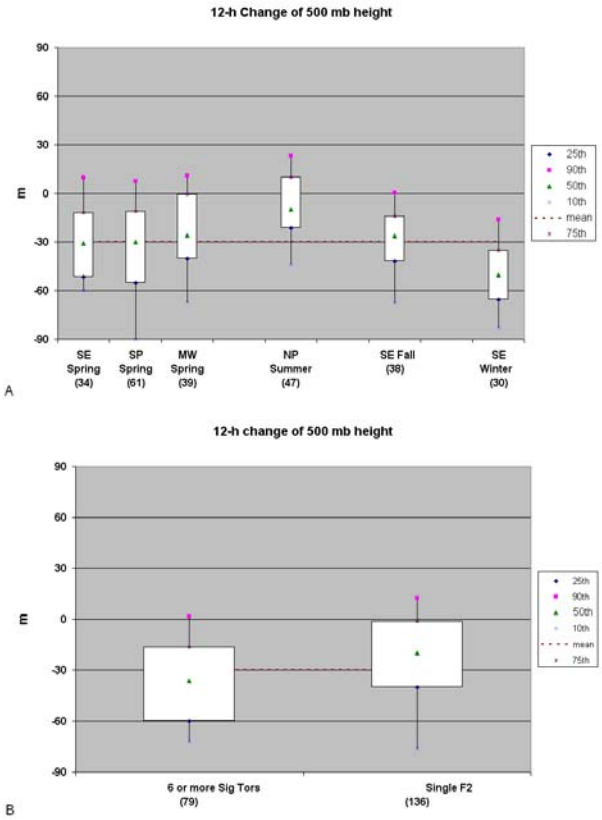

Figure 11. Same as in Fig. 8, except for the change in 500 hPa height in the 12-h period preceding significant tornado cases by a) region and season, and b) for cases with 6 or more significant tornadoes versus a single F2/EF2.wind speed.

The mean change in 500 (850) hPa temperatures was 0.2° (0.9°) C from 12-h prior to initial tornado time. Figures 14a and 14b depict essentially neutral thermal change in the mid-levels directly over the significant tornado locations and only slight warming in the low-levels, with relatively minor variations in the median noted amongst regions and seasons. In the spring, Southern Plains 700 hPa temperatures are noticeably warmer than over the Midwest or Southeast, reflecting the elevated mixed layer source region over the plateau (upstream from the Plains). Given the similar 500 hPa temperatures over the three regions in the spring, the warmer 700 hPa temperatures infer steeper mid level temperature lapse rates over the Southern Plains in the spring. The distribution of Southeast 500 hPa temperatures in the fall is similar (although broader) to the Northern Plains summer, though the much warmer 700 hPa temperatures over the Northern Plains are consistent with steeper mid level temperature lapse rates in the Northern Plains summer compared to the Southeast fall.

Maddox and Doswell (1982) hypothesized that pronounced low-level warm advection occurring in regions of strong conditional instability is a key component to the production of intense severe events, when mid-level vorticity patterns are weak. Our data suggest it is low-level moistening that plays a larger role than low-level warming in significant tornado events. This finding is important, since changes in lifted parcel moisture have approximately twice the impact on CAPE as temperature (e.g., Crook 1996).

The mean surface temperature (dew point) for all events was 75° (67°) F. Although the distribution of surface temperatures varies greatly based on season (Fig. 15a), dew points depict much less variation (Fig. 15b). The distribution of temperatures and dew points for events with 6 or more significant tornadoes was quite

similar to those events with a singular F2 or EF2 (Figs. 16a and 16b). Low-level moisture can be augmented along synoptic and mesoscale boundaries, or by local moisture sources, especially during the warm season in the Plains. However, the background synoptic regime is likely the largest contributor to low-level moisture distributions through horizontal advection from the relatively warm ocean source regions.

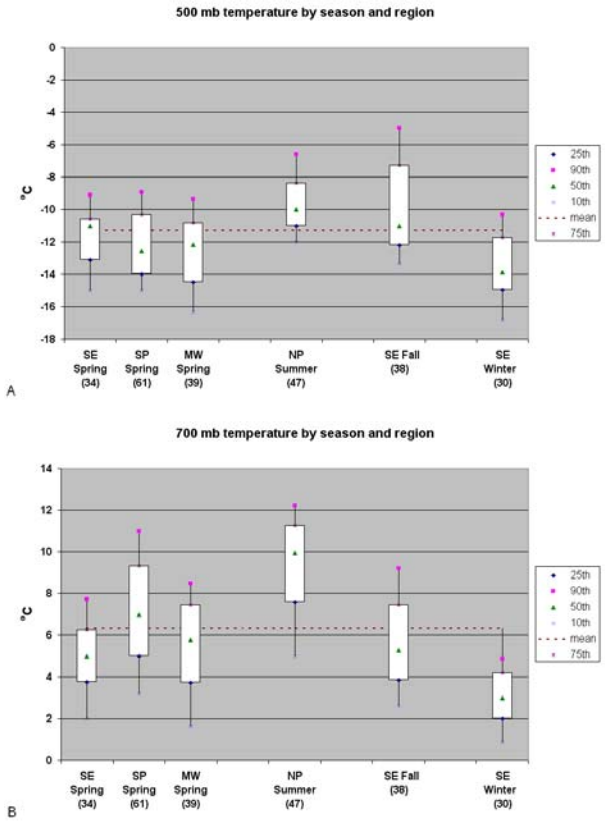

Figure 12. Box and whiskers plot of temperatures by region and season for a) 500 hPa and b) 700 hPa. Plotting conventions are the same as Fig. 8.

iii) Miller checklist comparison

A modified version of the Miller (1972) severe weather checklist utilizing percentile rank distributions is provided in Table 4, which lists only the variables included in our case sample. Our significant tornado outbreak cases were consistent with Miller's "strong" category for the magnitude of the low- and mid-tropospheric flow, low-level and surface dew point temperatures, as well as for surface pressure and 12-h pressure falls. Weaker winds in the "moderate" category characterized the upper-level flow, along with low- and mid-tropospheric flow for singular significant tornado cases. Median 500 hPa 12-h height changes fell in Miller's "moderate" category for our significant tornado outbreaks, and in the "weak" category for the singular F2/EF2 events. Operational forecasters have tended to focus on the more intense synoptic systems as the greatest threat to produce a significant tornado outbreak. However, our relatively small 500 hPa height falls in the area of the tornadoes (not to be confused with potentially larger height falls upstream) suggest that too much emphasis may be placed on the degree of synoptic "forcing", and weaker forcing may actually favor discrete cell development and a greater threat for tornadoes (Thompson and Edwards 2000).

c) Influence of synoptic boundaries

Surface boundaries were identified in this work via standard plots of first order observing stations. Given the standard station spacing on the order of 50 km, precise boundary locations cannot be known, and smaller-scale boundaries may have gone undetected in this sample of cases. Storm initiation with respect to surface boundaries reveals a tendency for discrete cell cases to initiate in the vicinity of drylines, pre-frontal troughs, and in the open warm sector (Fig. 17a), in agreement with the findings of Dial et al. (2008). In contrast, a larger percentage of QLCSs formed along cold fronts or pre-frontal troughs. Relatively few QLCSs formed along drylines, warm fronts, or outflow boundaries.

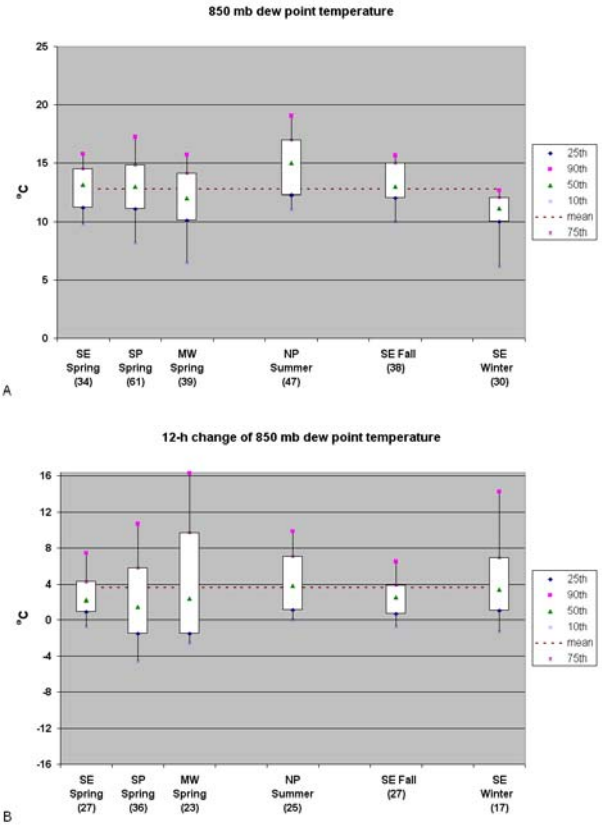

Figure 13. Box and whiskers plot of 850 hPa dew point by region and season at 1) the time of the event, and b) 12-h change preceding the event. Plotting conventions are the same as Fig. 8

Boundary types varied markedly from storm initiation to later storm-boundary interaction. Roughly 30% of both QLCS and discrete cells, and 25% of the clusters, appeared to move along or across a surface warm (or stationary) front near the time of the significant tornado reports (Fig. 17b). Storm interactions with pre-existing (mesoscale) outflow boundaries accounted for another 5-10% of the cases, while ~55-65% of the significant tornado cases occurred in the open warm sector with no apparent boundary interactions. Markowski et al. (1998) found a larger percentage (~70%) of storm-boundary interactions with F1-F4 tornadoes observed during the VORTEX field project across the southern Plains in the spring of 1995. Their sample of events did not focus solely on significant (F2+) tornadoes and included only a single tornado "cluster" outbreak on 8 June 1995 at the end of the project. Several of the most intense and longest-lived tornadoes on 8 June 1995 did not appear to be associated with any pre-existing mesoscale or storm-scale boundaries. An examination by F-scale damage ratings reveals that storm-boundary interactions were probable in 37% of our 30 F4-F5 cases, and 44% of our 329 F2-F3 cases.

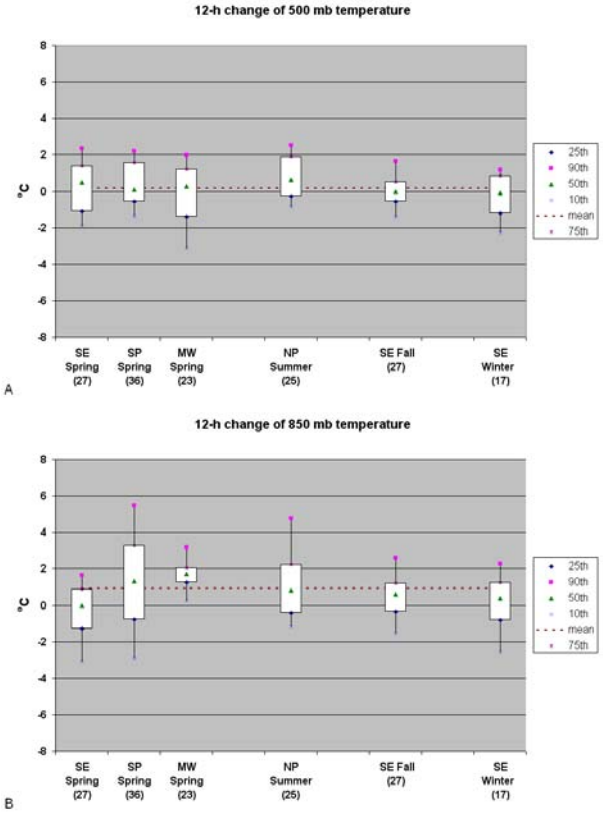

Figure 14. Box and whiskers plot of the change in temperature in the 12-h period preceding significant tornado events by region and season at 1) 500 hPa and b) 850 hPa. Plotting conventions are the same as Fig. 8.

Lastly, stratifying by the total number of significant tornadoes during the convective day yielded some relative comparisons between the isolated event cases and those that were part of a larger tornado outbreak. Using the arbitrary thresholds of a single F2+ tornado to identify isolated events (136 cases), and six or more F2+ tornadoes as a larger outbreak (79 cases), it was apparent that a larger percentage of boundary interaction cases comprised the isolated event sample (46%) versus the outbreak sample (33%). Differences in the actual fraction of boundary interactions with each individual tornado and storm mode will likely be more pronounced than represented by our sample of cases.

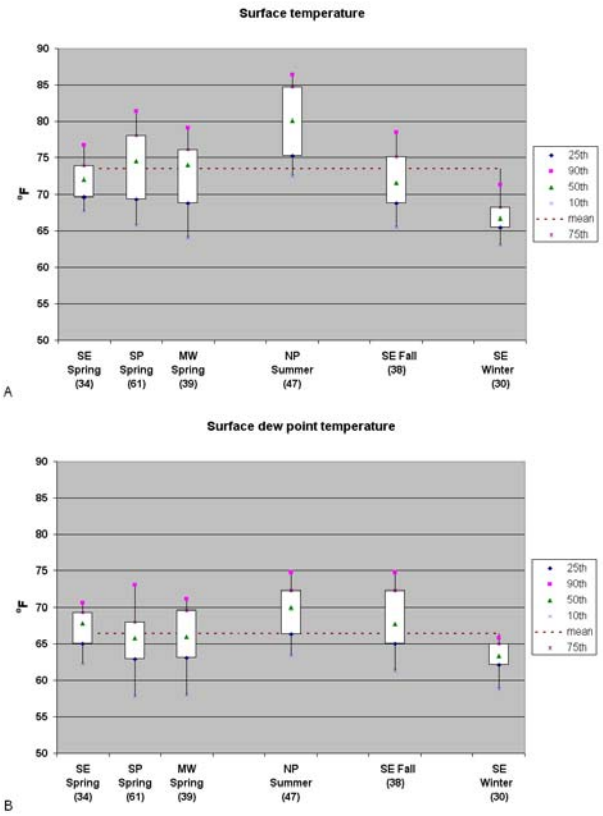

Figure 15. Box and whiskers plot by region and season of a) surface temperature and b) surface dew point temperature. Plotting conventions are the same as Fig. 8.

4. SUMMARY AND DISCUSSION

A sample of significant tornado (F2+ damage) cases and associated convective mode was collected for the eight year period from January 2000 through December 2007, based on Storm Data reports and regional radar reflectivity mosaic images. Significant tornadoes were most common with discrete cells (64% of cases, 74% of total tornadoes), while QLCSs accounted for 25% of our cases (18% of total tornadoes). An intermediate "cluster" category contained the remaining 11% of our cases. Significant tornadoes occurred most frequently with discrete cells in the spring (southern Plains) and summer (northern Plains), while QLCS significant tornadoes were more evenly distributed through the year. Significant

Table 4. Percentile rank distributions of selected parameters for comparison to Miller's (1972) Summary of Key Parameters for severe weather outbreaks.

Parameter	Percentile				
	10th	25th	50th	75th	90th
300 hPa Wind Speed (kt)	36	48	62	75	90
500 hPa Wind Speed (kt)	34	41	51	60	70
850 hPa Wind Speed (kt)	20	28	35	44	50
12-h 500 hPa Height Change (m)	+10	-7	-27	-50	-77
850 hPa Dew Point (°C)	8	11	13	15	16
Surface Dew Point (°F)	59	63	67	70	73
12-h Surface Pressure Falls (hPa)	1	3	5	7	9
Surface Pressure (hPa)	997	1001	1005	1008	1011

tornadoes were almost equally probable with discrete cells and QLCSs in the southeast states during the winter and spring. The discrete cell cases displayed a clear diurnal peak near 00 UTC and a minimum a few hours before sunrise. A muted peak in QLCS tornadoes was noted around 00UTC during the warm season (Apr-Oct), with a secondary peak around 09 UTC (near the time of diurnal minimum in discrete cell tornadoes). The relative peak in QLCS significant tornado cases near 09 UTC was present during both the warm season and cool season (Nov-Mar). This suggests that the most difficult tornado forecasts associated with convective mode are during the winter in the southeast, while significant tornadoes occur most consistently with discrete cells across the southern Plains during the evening in the spring. Meanwhile, the largest tornado outbreaks were dominated by discrete cell tornadoes (79%), and QLCS cases were a greater fraction of the singular F2/EF2 events (33%).

We have largely replicated the results of prior studies that focused on pattern recognition and mandatory pressure level data (e.g., Miller 1972; David 1976). Lower and middle tropospheric temperatures in significant tornado cases tended to increase in concert with general warming from the cool season into the warm season, with the warmest temperatures and dew point temperatures observed during the northern Plains summer, and the coolest during the winter in the

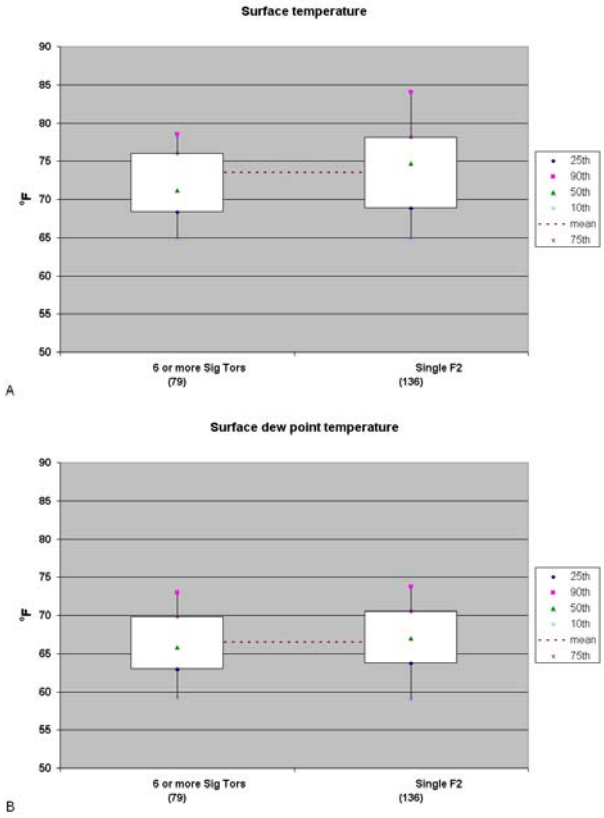

Figure 16. Same as in Fig. 15, except for cases with six or more significant tornadoes versus a single F2/EF2.

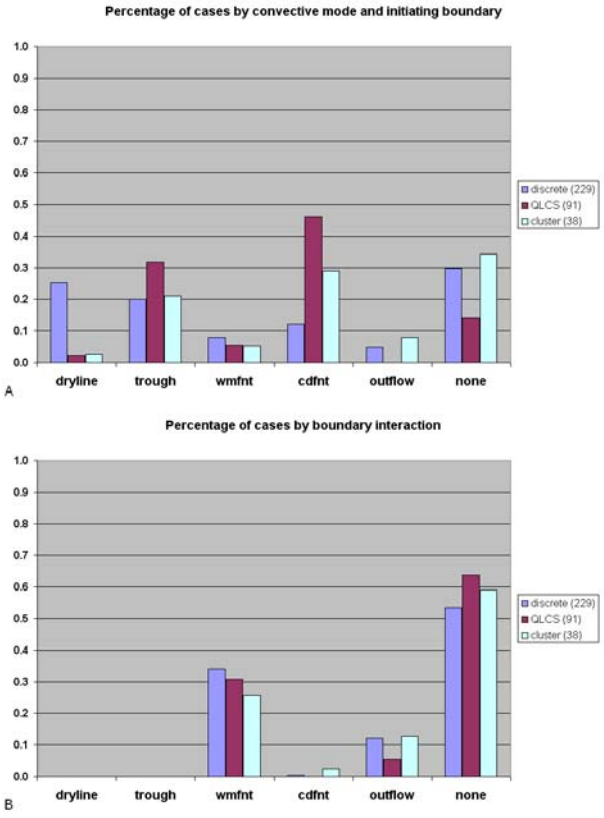

Figure 17. Relative frequency of convective modes for significant tornado cases by 1) initiating surface boundary, and b) storm-boundary interactions.

southeastern states. More notable differences with the 1970s studies include greater values of low-level moisture and wind speed, which are likely attributable to different sampling criteria (significant tornadoes versus all tornadoes) increased temporal and spatial resolution of the hourly RUC analyses compared to synoptic observations utilized in many previous studies.

Temperature changes aloft (e.g., 500 hPa) were rather small in the 12-h period leading up to the tornado cases. Local moistening of roughly 2-4o C in the low levels was documented in the 12-h period leading up to the significant tornado cases. Surprisingly, 500 hPa 12-h height changes were typically around 30 m in the immediate area of the significant tornado cases. Operational forecasters have tended to focus on the more intense and rapidly moving synoptic systems, with larger resultant change fields, when attempting to forecast significant tornado episodes. The synoptic systems associated with significant tornado cases vary from barely perceptible to high-amplitude waves, but the degree of "forcing" for large scale ascent in the low-mid levels (often referred to informally as "dynamics") does not need to be large directly over the area of the significant tornadoes. The success of pattern recognition in tornado forecasting is largely a function of how consistently the identified pattern relates to the generation and co-location of the necessary ingredients for significantly tornadic supercells, which account for the largest percentage of significant tornado events and outbreaks.

A few previous studies have examined tornado occurrence with storms interacting with surface boundaries. Roughly 35-45% of our tornado cases involved potential storm and surface boundary interactions, whereas almost 70% of the tornadoes observed during VORTEX-95 were the result of boundary interactions. Surface warm (stationary) fronts and residual convective outflow boundaries accounted for almost all of the boundary interactions, though a majority of our cases appeared to occur in the open warm sector of synoptic cyclones where no boundaries were apparent in standard surface observing networks. This difference in relative frequencies of significant tornadoes along boundaries is likely attributable to the narrow range of climatic regimes that characterized the VORTEX-95 cases in the southern Plains in the spring. A slight majority of significant tornadoes occurred in the absence of synoptic fronts or outflow boundaries in all seasons combined across the continental United States, which suggests that the background synoptic regime can be the dominant contributor to the necessary ingredients for many significant tornado episodes (e.g., low-level shear provided by large scale flow regime, as opposed to mesoscale augmentation along a residual outflow boundary). Further, some tendency was noted for boundary interactions to account for a larger percentage of isolated significant tornado cases (46%, a single F2+ tornado) compared to cases that were part of larger tornado outbreaks (33%, 6 or more F2+ tornadoes). Our case selection criteria likely skewed our case sample away from the larger tornado outbreaks because multiple tornadoes with the same storm mode (e.g., discrete cells in the open warm sector) comprised a substantial fraction of the total tornado events. The relative frequency of synoptic and mesoscale boundary interactions in the larger tornado outbreaks is likely lower than presented here, since our case selection criteria did not include multiple significant tornadoes with the same convective mode (e.g., several discrete cells producing multiple significant tornadoes in the open warm sector counted as one case). More detailed surface observations, satellite imagery, radar imagery, and specific counts of individual tornadoes by boundary interaction type will be necessary to fully establish the relative frequencies of tornadoes with and without boundary interactions.

ACKNOWLEDGEMENTS:

The authors thank Heather Moser with the University of Oklahoma for her assistance in creating scripts to decode RUC grib files and extract point data for individual events, as well as Steve Weiss (SPC) for reviewing the initial manuscript and Linda Crank for handling the "desktop publishing" aspects of preparing conference preprint papers.

REFERENCES

Benjamin, S. G., and Coauthors, 2004: An hourly assimilation-forecast cycle: The RUC. Mon. Wea. Rev., 132, 495-518.

Bluestein, H. B., 1999: A history of severe-storm-intercept field programs. Wea. Forecasting, 14, 558-577.

Crook, N. A., 1996: Sensitivity of moist convection forced by boundary layer processes to low-level thermodynamic fields. Mon. Wea. Rev., 124, 1767-1785.

David, C. L., 1976: A study of upper air parameters at the time of tornadoes. Mon. Wea. Rev., 104, 546-551.

Davies-Jones, R., R. J. Trapp, and H. B. Bluestein, 2001: Tornadoes and tornadic storms. Severe Convective Storms, Meteor. Monogr., No. 50, Amer. Meteor. Soc., 167-222.

Dial, G. L., J. P. Racy, and R. L. Thompson, 2008: Nowcasting convective mode evolution along synoptic boundaries. Submitted to Wea. Forecasting.

Doswell, C. A. III, and D. W. Burgess, 1988: Some issues of United States tornado climatology. Mon. Wea. Rev., 116, 495-501.

_____, H. E. Brooks, and R. A. Maddox, 1996: Flash flood forecasting: An ingredients-based methodology. Wea. Forecasting, 14, 338-345.

Fawbush, E., J, R. C. Miller, and L. G. Starrett, 1951: An empirical method of forecasting tornado development. Bull. Amer. Meteor. Soc., 32, 1-9.

Galway, J. G., 1992: Early severe thunderstorm forecasting and research by the United States Weather Bureau. Wea. Forecasting, 7, 564-587.

Grams, J. S., W. A. Gallus, Jr., S. E. Koch, L. S. Wharton, A. Loughe, and E. E. Ebert, 2006: The use of a modified Ebert-McBride technique to evaluate mesoscale model QPF as a function of convective system morphology during IHOP 2002. Wea. Forecasting, 21, 288–306.

Johns, R. H., and C. A. Doswell III, 1992: Severe local storms forecasting. Wea. Forecasting, 7, 588-612.

_____, J. M. Davies, and P. M. Leftwich, 1993: Some wind and instability parameters associated with strong and violent tornadoes. Part II: Variations in the combinations of wind and instability parameters. The Tornado: Its Structure, Dynamics, Hazards, and Prediction. Geophys. Monogr., No. 79, Amer. Geophys. Union, 583-590.

Maddox, R.A. and C.A. Doswell III, 1982: An examination of jet stream configurations, 500 mb vorticity advection and low level thermal advection patterns during extended periods of intense convection. Mon. Wea. Rev., 110, 184-197.

Markowski, P. M., E. N. Rasmussen, and J. M. Straka, 1998: The occurrence of tornadoes in supercells interacting with boundaries during VORTEX-95. Mon. Wea. Rev., 13, 852-859.

_____, C. Hannon, J. Frame, E. Lancaster, A. Pietrycha, R. Edwards, and R. L. Thompson, 2003: Characteristics of vertical wind profiles near supercells obtained from the Rapid Update Cycle. Wea. Forecasting, 18, 1262-1272.

Miller, R. C., 1972: Notes on analysis and severe-storm forecasting procedures of the Air Force Global Weather Central. Air Weather Service Tech. Rep. 200 (Rev.), Air Weather Service, Scott Air Force Base, IL, 190 pp.

Moller, A. R., 2001: Severe local storms forecasting. Severe Convective Storms, Meteo. Monogr., No. 50, Amer. Meteor. Soc., 433-480.

Rasmussen, E. N., and D. O. Blanchard, 1998: A baseline climatology of sounding-derived supercell and tornado forecast parameters. Wea. Forecasting, 13, 1148-1164.

_____, 2003: Refined supercell and tornado forecast parameters. Wea. Forecasting, 18, 530-535.

Schaefer, J. T., 1986: Severe thunderstorm forecasting: A historical perspective. Wea. Forecasting, 1, 164-189.

Thompson, R. L., and R. Edwards, 2000: An overview of environmental conditions and forecast implications of the 3 May 1999 tornado outbreak. Wea. Forecasting, 15, 682-699.

_____, _____, J. A. Hart, K. L. Elmore, and P. Markowski, 2003: Close proximity soundings within supercell environments obtained from the Rapid Update Cycle. Wea. Forecasting, 18, 1243-1261.

_____, and C. M. Mead, 2006: Tornado failure modes in central and southern Great Plains severe thunderstorm episodes. Preprints, 23rd Conf. Severe Local Storms, St. Louis MO.

Trapp, R. J., S. A. Tessendorf, E. S. Godfrey, and H. E. Brooks, 2005: Tornadoes from squall lines and bow echoes: Part I: Climatological distribution. Wea. Forecasting, 20, 23-33.

Uccellini, L. W., and D. R. Johnson, 1979: The coupling of upper and lower tropospheric jet streaks and implications for the development of severe convective storms. Mon. Wea. Rev., 107, 682-703.

Wilhelmson, R. B., and L. J., Wicker, 2001: Numerical modeling of severe local storms. Severe Convective Storms, Meteo. Monogr., No. 50, Amer. Meteor. Soc., 123-166.

Winston, J. S., 1956: Forecasting tornadoes and severe thunderstorms. Forecasting Guide No. 1, U. S. Weather Bureau, Washington, D. C., 34 pp.